

Intra-operative 3D Guidance in Prostate Brachytherapy Using a Non-isocentric C-arm*

A. Jain^{1,3}, A. Deguet¹, I. Iordachita¹, G. Chintalapani¹, J. Blevins², Y. Le¹,
E. Armour¹, C. Burdette², D. Song¹, and G. Fichtinger¹

¹ Johns Hopkins University

² Acoustic MedSystems Inc.

³ Philips Research North America

Abstract. Intra-operative guidance in Transrectal Ultrasound (TRUS) guided prostate brachytherapy requires localization of inserted radioactive seeds relative to the prostate. Seeds were reconstructed using a typical C-arm, and exported to a commercial brachytherapy system for dosimetry analysis. Technical obstacles for 3D reconstruction on a non-isocentric C-arm included pose-dependent C-arm calibration; distortion correction; pose estimation of C-arm images; seed reconstruction; and C-arm to TRUS registration. In precision-machined hard phantoms with 40-100 seeds, we correctly reconstructed 99.8% seeds with a mean 3D accuracy of 0.68 mm. In soft tissue phantoms with 45-87 seeds and clinically realistic 15° C-arm motion, we correctly reconstructed 100% seeds with an accuracy of 1.3 mm. The reconstructed 3D seed positions were then registered to the prostate segmented from TRUS. In a Phase-1 clinical trial, so far on 4 patients with 66-84 seeds, we achieved intra-operative monitoring of seed distribution and dosimetry. We optimized the 100% prescribed iso-dose contour by inserting an average of 3.75 additional seeds, making intra-operative dosimetry possible on a typical C-arm, at negligible additional cost to the existing clinical installation.

1 Introduction

With an approximate annual incidence of 220,000 new cases and 33,000 deaths (United States) prostate cancer continues to be the most common cancer in men. Transrectal Ultrasound (TRUS) guided permanent low-dose-rate brachytherapy (insertion of radioactive seeds into the prostate) has emerged as a common & effective treatment modality for early stage low risk prostate cancer, with an expected 50,000 surgeries every year. The success of brachytherapy (i.e. maximizing its efficacy while minimizing its co-morbidity) chiefly depends on our ability to tailor the therapeutic dose to the patient's individual anatomy. The main limitation in contemporary brachytherapy is intra-operative tissue expansion (edema), causing incorrect seed placement, which may potentially lead to insufficient dose to the cancer and/or excessive radiation to the rectum, urethra, or bladder. The former might permit the cancer to relapse, while the latter

* Supported by DoD PC050170, DoD PC050042 and NIH 2R44CA099374.

causes adverse side effects like rectal ulceration. According to a comprehensive review by the American Brachytherapy Society [1], *the pre-planned technique used for permanent prostate brachytherapy has limitations that may be overcome by intra-operative planning.*

Prostate brachytherapy is almost exclusively performed under TRUS guidance. Various researchers have tried to segment the seeds from TRUS images by linking seeds with spacers, using X-rays to initialize segmentation, using vibro-acoustography or transurethral ultrasound as a new imaging modality, or segmenting them directly in TRUS images by using corrugated seeds that are better visible than conventional ones [2]. But even when meticulously hand-segmented, up to 25% of the seeds may remain hidden in ultrasound. C-arms are also ubiquitous, though used only for gross visual assessment of the implanted seed positions (approximately 60% of the practitioners using it in the operating room [3]). In spite of significant efforts that have been made towards computational fluoroscopic guidance in general surgery [4], C-arms cannot yet be used for intra-operative brachytherapy guidance due to a plethora of technical limitations. While several groups have published protocols and clinical outcomes favorably supporting C-arm fluoroscopy for intra-operative dosimetric analysis [5,6,7], this technique is yet to become a standard of care across hospitals. In this paper we report a system to reconstruct 3D seed positions (visible in X-ray) and spatially register them to the prostate (visible in TRUS). Our **primary contribution** is our ability to use any typical non-isocentric uncalibrated C-arm present in most hospitals, in comparison to the use of calibrated isocentric machines [5,6] or an approximate reconstruction [7], as reported in the literature.

2 Methods and Materials

The system is designed to easily integrate with commercial brachytherapy installations. We employ a regular clinical brachytherapy setup, without alteration, including a treatment planning workstation & stabilizer/stepper (Interplant[®], CMS, St Louis), TRUS (B&K Medical Pro Focus) and a C-arm (GE OEC

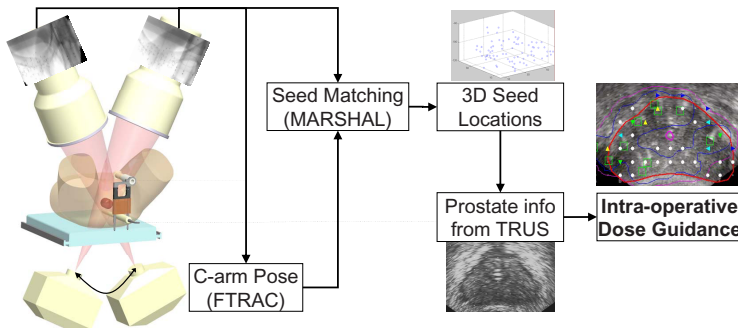


Fig. 1. Overview of the proposed solution. The FTRAC fiducial tracks C-arms, and also registers TRUS to C-arm images, making quantitative brachytherapy possible.

98/9900). The C-arm is interfaced with a laptop through an NTSC video line and frame grabber, making the image capture independent of the C-arm model.

Workflow: The clinical workflow (Fig. 1) is identical to the standard procedure until the clinician decides to run a reconstruction and optimization. A set of C-arm images are collected with *a separation as wide as clinically possible* ($10-15^\circ$ around AP-axis) and synchronously transferred to the laptop. After processing the images, the seeds are reconstructed and exported to the Interplant[®] system. The physician uses standard Interplant[®] tools to analyze, optimize and modify the remainder of the plan. The procedure concludes when the exit dosimetry shows no cold spots (under-radiated locations).

Numerous technical obstacles have to be overcome to realize C-arm based intra-operative dosimetry: (a) C-arm calibration; (b) image distortion correction; (c) pose estimation of C-arm images; (d) seed reconstruction; (e) registration of C-arm to TRUS; (f) dosimetry analysis; and finally (g) implant optimization. We have developed a system that overcomes these limitations in providing quantitative intra-operative dosimetry. In what follows, we will describe briefly each component of the system, skipping the mathematical framework for lack of space.

C-arm Source Calibration and Image Distortion: Since both C-arm calibration and distortion are pose-dependent, contemporary fluoroscopy calibrates/distortion-corrects at each imaging pose using a cumbersome calibration-fixtured, which is a significant liability. Our approach is a complete departure. Using a mathematical & experimental framework, we demonstrated that calibration is not critical for prostate seed reconstruction. Just an approximate pre-operative calibration suffices [8]. The central intuition is that object reconstruction using a mis-calibrated C-arm changes only the absolute positions of the objects, but not their relative ones (Fig. 2). Additionally, statistical analysis of the distortion in a 15° limited workspace around the AP-axis revealed that just a pre-operative correction can reduce the average distortion from 3.31 mm to 0.51 mm, sufficient for accurate 3D reconstruction. The numbers are expected to be similar for other C-arms too.

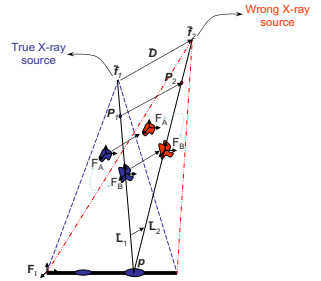


Fig. 2. Mis-calibration conserves relative reconstruction between objects A and B (eg. seeds)

Pose Estimation: The most critical component for 3D reconstruction is C-arm pose estimation. C-arms available in most hospitals do not have encoded rotational joints, making the amount of C-arm motion unavailable. C-arm tracking using auxiliary trackers is expensive, inaccurate in the presence of metal (EM tracking) or intrudes in the operating room (optical tracking). There has been some work on fiducial based tracking, wherein a fiducial (usually large for accuracy) is introduced in the X-ray FOV and its projection in the image encodes the

6 DOF pose of the C-arm. We proposed a new fluoroscope tracking (FTRAC) [9] fiducial design that uses an ellipse (key contribution), allowing for a small (3x3x5cm) yet accurate fiducial. In particular, the small size makes it easier to be always in the FOV & to be robust to image distortion. Extensive phantom experiments indicated a mean tracking accuracy on distorted C-arms of 0.56 mm in translation and 0.25° in rotation, an accuracy comparable to expensive external trackers.

Seed Segmentation: We developed an automated seed segmentation algorithm that employs the morphological top-hat transform to perform the basic seed segmentation, followed by thresholding, region labeling, and finally a two-phase classification to segment both single seeds & clusters. The result of the segmentation is verified on the screen to allow for a manual bypass by the surgeon.

Seed Correspondence & Reconstruction: The 3D coordinates of the implanted seeds can now be triangulated by resolving the correspondence of seeds in the multiple X-ray images. We formalized seed correspondence to a network-flow-based combinatorial optimization, wherein the desired solution is the flow with minimum cost. Using this abstraction, we proposed an algorithm (MARSHAL [10]) that runs in cubic-time using any number of images. In comparison, previous solutions have predominantly been heuristic explorations of the large search space (10^{300}). In addition, the framework also robustly resolves all the seeds that are hidden in the images (typically 4-7% due to the high density). MARSHAL typically reconstructs 99.8% of the seeds and runs in under 5s in MATLAB (a 95% minimum-detection-rate is usually deemed sufficient [11]).

Registration of C-arm to TRUS: The FTRAC is attached to the needle-insertion template by a precisely machined mechanical connector (Fig. 4) in a known relative way (pre-calibration). The template has already been calibrated to TRUS as per the usual clinical protocol. Thus a simple application of the various known frame transformations, registers the 3D seeds (FTRAC) to the prostate (TRUS).

System Implementation, Dosimetry Analysis and Implant Optimization:

We have integrated all the above functions into a MATLAB program with a GUI. The package runs on a laptop that sends reconstructed seed positions (in template coordinates) to the Interplant[®] system. In order to not require a new FDA approval, we maintain the integrity of the FDA-approved Interplant[®] by not modifying the commercial software, and instead use a text file to export the 3D seed locations.

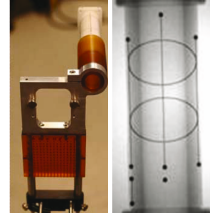


Fig. 3. The FTRAC fiducial mounted over the seed-insertion needle template using a mechanical connector. An X-ray image of the same.

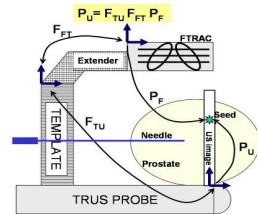


Fig. 4. FTRAC & template pre-calibration using a rigid mount

The physician uses standard Interplant[®] tools (isodose coverage, etc.) for dose analysis, and if needed, modifies the residual plan to avoid hot spots or fill in cold spots. This process can be repeated multiple times during the surgery.

3 Phantom Experiments and Results

We have extensively tested the system and its components in various phantoms and in an ongoing Phase-1 clinical trial. To do so, we introduce the terms **absolute** and **relative** reconstruction errors. Using X-ray images, the seeds are reconstructed with respect to (w.r.t.) the FTRAC frame. In experiments where the ground truth location of the seeds w.r.t. the FTRAC is known, the comparative analysis is called absolute accuracy. Sometimes (eg. in patients), the true seed locations w.r.t. the FTRAC are not available and the reconstruction can only be compared to the seeds extracted from post-op data (using a rigid point-cloud transform), in which case the evaluation is called relative accuracy.

Solid Seed Phantom: An acetol (Delrin) phantom consisting of ten slabs (5mm each) was fabricated (Fig. 5 (a)). This phantom provides a multitude of implants with sub-mm ground truth accuracy. The fiducial was *rigidly* attached to the phantom in a known way, establishing the accurate ground truth 3D location of each seed. Realistic prostate implants (1.56 seeds/cc, 40-100 seeds) were imaged within a 30° cone around the AP-axis. The true correspondence was manually established by using the 3D locations, known from the precise fabrication. Averaged results indicate that we correctly match 98.5% & 99.8% of the seeds using 3 & 4 images (100 & 75 total trials) respectively. The mean 3D absolute reconstruction accuracy was 0.65 mm (STD 0.27 mm), while the relative accuracy was 0.35 mm. Furthermore, using 4 images yielded only one poorly mis-matched seed from the 75 datasets, suggesting the use of 4 images for better clinical guidance.

Soft Training Phantoms: We fully seeded three standard prostate brachytherapy phantoms (Fig. 5 (b)) with realistic implant plans (45, 49, 87 seeds). Seed

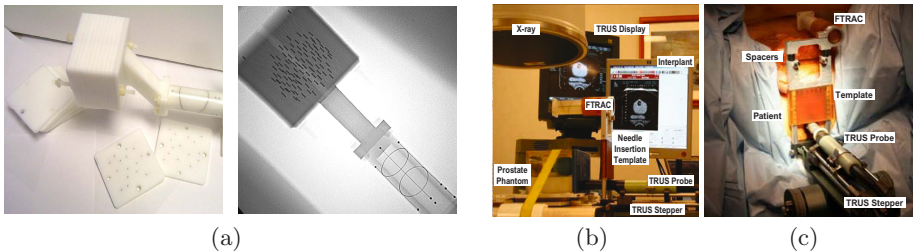


Fig. 5. (a) An image of the solid seed phantom attached to the fiducial with a typical X-ray image of the combination. (b) An annotated image of the experimental setup for the training phantom experiment. (c) The clinical setup from the Phase-I clinical trial.

locations reconstructed from fluoro using realistic (maximum available clinically) image separation (about 15°) were compared to their corresponding ground truth locations segmented manually in CT (1mm slice thickness). Additionally, the 45 & 87-seed phantoms were rigidly attached to the FTRAC, providing the absolute ground truth (from CT). The 49-seed phantom was used to conduct a full scale practice-surgery, in which case the 3D reconstruction could be compared only to the seed cloud from post-op CT (without FTRAC), providing just relative accuracy. *Note that our reconstruction accuracy (as evident from the previous experiments) is better than the CT resolution.* The absolute reconstruction errors for the 45, 87-seed phantoms were 1.64 mm & 0.95 mm (STD 0.17 mm), while the relative reconstruction errors for the 45, 49, 87-seed phantoms were 0.22 mm, 0.29 mm, 0.20 mm (STD 0.13 mm). A mean translation shift of 1.32 mm was observed in the 3D reconstructions, predominantly due to the limited C-arm workspace (solid-phantom experiments with 30° motion have 0.65 mm accuracy). It was observed that the shift was mostly random & not in any particular direction. Nevertheless, the accuracy is sufficient for brachytherapy, especially since a small shift still detects the cold spots.

Patients: A total of 11 batches of reconstructions were carried out on 4 patients with 2 – 3 batches/patient & 22 – 84 seeds/batch. Since the seeds migrate by the time a post-operative CT is taken, there is no easy ground truth for real patients. Hence, for each reconstruction, 5 – 6 additional X-ray images were taken. The reconstructed 3D seed locations were projected on these additional images and compared to their segmented corresponding 2D locations. The results from 55 projections gave a 2D mean error of 1.59 mm (STD 0.33 mm, max 2.44 mm), indicating a sub-mm 3D accuracy (errors get magnified when projected).

Registration Accuracy: To measure the accuracy of the fiducial to template registration, three batches of five needles each were inserted randomly at random depths into the template. Their reconstructed tip locations were then compared to their true measured locations (both in template coordinates). The limited-angle image-capture protocol was kept similar to that used in the clinic. The average absolute error (reconstruction together with registration) was 1.03 mm (STD 0.20 mm), while the average relative error was 0.36 mm (STD 0.31 mm), with an average translation shift of 0.97 mm.

System Accuracy: To measure the full system error, 5 needles (tips) were inserted into a prostate brachytherapy training phantom, reconstructed in 3D and exported to the Interplant[®] software. Manual segmentation of the needles in TRUS images (sagittal for depth and transverse for X-Y) provided ground truth. The mean absolute error for the 5 needle tips was 4 mm (STD 0.53 mm), with a translation shift of 3.94 mm. In comparison, the relative error for the complete system was only 0.83 mm (STD 0.18 mm). The shift can mainly be attributed to a bias in the Template-TRUS pre-calibration (~ 3 mm) done as part of current clinical practice, & in the 3D reconstruction (~ 1 mm). Nevertheless, we

removed this shift in the clinical cases by applying a translation-offset to the reconstructed X-ray seed coordinates. This offset was intra-operatively estimated by comparing the centroid of the reconstructed seeds with that of the planned seed locations, and by aligning the two together. Note that the centroid is a first-order statistic and robust to any spatially symmetric noise/displacement model. Though a heuristic, it provided excellent qualitative results according to the surgeon, who read the visual cues at the reconstructed seed locations in TRUS images. Based on the experiments so far and the surgeon’s feedback, the overall accuracy of the system is expected to be 1 – 2 mm during clinical use.

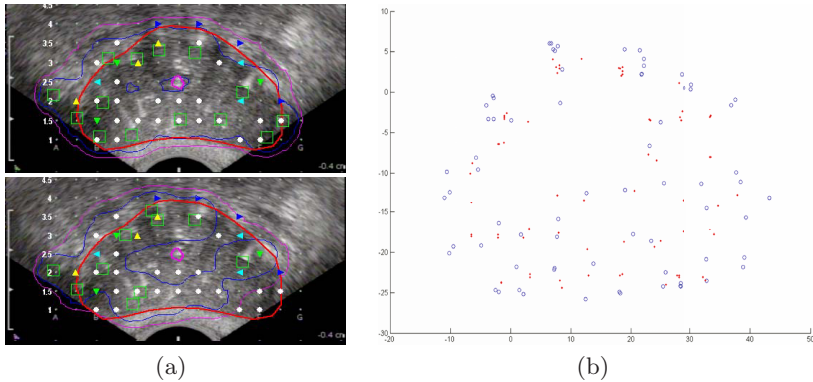


Fig. 6. (a) The system is able to detect cold spots. The 100% iso-dose contours (pink) as assumed by the planning system (top) and as computed by the proposed system (bottom), discovering 2 cold spots. Red marks the prostate boundary. The green squares delineate the seed coordinates, detecting 4 seeds that had drifted out of slice. (b) The system can visualize intra-operative edema (mean 4.6 mm, STD 2.4 mm, max 12.3 mm). The ‘planned’ (red) versus the ‘reconstructed’ (blue) seed positions as seen in the template view. A trend of outward radiation from their initial locations is observed.

Phase-I Clinical Trial: We have treated 4 patients so far (Fig. 5 (c)), out of a total of 6 that will be enrolled. Intra-operative dosimetry was performed halfway during the surgery, at the end, and after additional seed insertions. The current protocol adds 15 minutes to the OR time for each reconstruction, including the capture of extra images (validation), reconstruction, and dosimetry optimization. In regular clinical practice, we anticipate the need for only a single exit-dosimetry reconstruction, increasing the OR time by about 10 minutes. *In all the patients the final dosimetry detected cold spots* (Fig. 6 (a)). The clinician grew quickly to trust the system in detecting cold spots, and instead minimized potential hot spots during the surgery. All patients were released from the operating room with satisfactory outcomes. *Intra-operative visualization of edema (prostate swelling) was also possible* (Fig. 6 (b)), which was found to be 0.73, 4.64, 4.59, 4.05 mm (STD 1.1, 2.2, 2.34, 2.37 mm). *The seeds (and hence the prostate) showed a clear tendency for outward migration from their drop positions (with maximums up to 15 mm).* Edema is the single largest factor that makes the perfect delivery

of the pre-planned dose nearly impossible. In almost all the patients, towards the end of the surgery, it was found that the apex of the prostate (surgeon-end) was under-dosed. The medical team found the intra-operative visualization of under-dosed regions valuable, inserting an additional 1, 2, 3, 9 seeds to make the 100% prescribed iso-dose contour cover the prostate. A further comparison of the exit implant to Day-0 CTs (2 mm slices) showed mean errors of 5.43, 6.16, 3.13, 5.15 mm (STD 2.46, 2.96, 2.02, 2.71 mm), indicating a further post-operative seed migration. Though, post-operative seed migration is an inherent limitation in brachytherapy, surgeons usually accommodate for it by slightly over-dosing the patient (note that sub-mm seed placement is non-critical). A study with 40 patients is currently being planned, to make a statistically relevant evaluation of the medical benefit of the system using clinical indicators.

4 Conclusion, Shortcomings and Future Work

A system for brachytherapy seed reconstruction has been presented, with extensive phantom and clinical trials. The absolute seed reconstruction accuracy from phantom trials is 1.3 mm using 15° C-arm motion, sufficient for detection of any cold spots. It shows usefulness and great potential from the limited Phase-1 patient trials. The system (a) requires no significant hardware; (b) does not alter the current clinical workflow; (c) can be used with any C-arm; & (d) integrates easily with any pre-existing brachytherapy installation, making it economically sustainable and scalable. There is some added radiation to the patient, though insignificant when compared to that from the seeds. Though not critical, primary shortcomings include (a) 15 minute additional OR time; (b) supervision during segmentation; & (c) a small translation bias. Furthermore, a TRUS based quantitative methodology is necessary to evaluate both the final system performance and clinical outcomes. Research is currently underway to remove these limitations, and to conduct a more detailed study using clinical indicators.

References

1. Nag, et al.: Intraoperative planning and evaluation of permanent prostate brachytherapy: report of the american brachytherapy society. IJROBP 51 (2001)
2. Tornes, A., Eriksen, M.: A new brachytherapy seed design for improved ultrasound visualization. In: IEEE Symposium on Ultrasonics, pp. 1278–1283. IEEE Computer Society Press, Los Alamitos (2003)
3. Prestidge, et al.: A survey of current clinical practice of permanent prostate brachytherapy in the united states. IJROBP 15, 40(2), 461–465 (1998)
4. Hofstetter, et al.: Fluoroscopy as an imaging means for computer-assisted surgical navigation. CAS 4(2), 65–76 (1999)
5. Reed, et al.: Intraoperative fluoroscopic dose assessment in prostate brachytherapy patients. Int. J. Radiat. Oncol. Biol. Phys. 63, 301–307 (2005)
6. Todor, et al.: Intraoperative dynamic dosimetry for prostate implants. Phys. Med. Biol. 48(9), 1153–1171 (2003)

7. French, et al.: Computing intraoperative dosimetry for prostate brachytherapy using trus and fluoroscopy. *Acad. Rad.* 12, 1262–1272 (2005)
8. Jain, et al.: C-arm calibration - is it really necessary? In: *SPIE Medical Imaging; Visualization, Image-Guided Procedures, and Display* (2007)
9. Jain, et al.: A robust fluoroscope tracking fiducial. *Med. Phys.* 32, 3185–3198 (2005)
10. Kon, R., Jain, A., Fichtinger, G.: Hidden seed reconstruction from c-arm images in brachytherapy. In: *IEEE ISBI*, pp. 526–529. IEEE Computer Society Press, Los Alamitos (2006)
11. Su, et al.: Examination of dosimetry accuracy as a function of seed detection rate in permanent prostate brachytherapy. *Med. Phy.* 32, 3049–3056 (2005)